

Synthesis and Electrochromic Properties of Two Random Copolymers Containing Benzotriazole, Benzothiadiazole as Electron Acceptors and Benzodithiophene or Indacenodithiophene as Electron Donors

Shaowen Pei¹, Xiuping Ju³, Jinsheng Zhao^{2,*}, Yan Wang, Hongmei Du^{2,*}

¹ Shandong Key Laboratory of Chemical Energy Storage and Novel Cell Technology, Liaocheng University, Liaocheng, 252059, P. R. China.

² Department of Chemistry and Chemical Engineering, Liaocheng University

³ College of Dongchang, Liaocheng University, Liaocheng University

Corresponding author, Tel: +86-635-8539607; Fax: +86-635-8539607.

*E-mail: j.s.zhao@163.com

Received: 2 March 2019/ Accepted: 22 April 2019 / Published: 10 June 2019

Two random copolymers, poly (benzotriazole-indacenodithiophene-benzothiadiazole) (PBTIDBD) and poly (benzotriazole-benzodithiophene-benzothiadiazole) (PBTBDBD) were synthesized and characterized by electrochemistry, spectroelectrochemistry, electrochromic switching, colorimetry and thermal gravimetric analysis. For PBTIDBD, the color of film changed from rosybrown in neutral state to transparent lightgrey in oxidized state. The band gap calculated according to the spectroelectrochemistry data is 1.86 eV, and the response time, optical contrast, coloration efficiency at 1560 nm are 1.04 s, 62.1%, 276.29 cm²·C⁻¹, respectively. And, for PBTBDBD, its color changes from rosybrown to transparent grey as it was fully oxidized. The band gap is 1.68 eV, and the response time, optical contrast, coloration efficiency at 1560 nm are 2.68 s, 62.4%, 193.31 cm²·C⁻¹, respectively. Both copolymers are stable at a high temperature, and the decomposition temperature of PBTIDBD and PBTBDBD are 463 °C and 326 °C. Both copolymers can be good candidates for electrochromic application.

Keywords: conducting polymers; indacenodithiophene; benzotriazole; benzothiadiazole; benzodithiophene.

1. INTRODUCTION

Electrochromic material is one kind of material with reversible color switch property when appropriate voltage is applied to the electrode, which is modified with the electrochromic material [1],

and has been developed widely during the past decades. It can be applied to many fields, such as display application, light emitting diodes [2], laser materials [3], organic light emitting diodes [4], polymer solar cells [5], and so on. The reason why electrochromic materials can attract so much attention is that it has many advantages, including supernal optical contrast [6, 7], high solubility in common organic solvents [8], high coloration efficiency [9], fast response time [10], good thermal stability [11], easy processability and low applied voltages [12].

Electrochromic conducting polymers consist of homopolymers, alternating copolymers and random copolymers. There are many kinds of π -conjugated polymers, including polyacetylene [13], polythiophene [14], polypyrrole [15], polyaniline [16], poly (paraphenylene) and their derivatives [17]. N. S. Sariciftci and his coworkers explained the mechanics of photoinduced electron transfer [18]. The charge carriers in conjugated polymers are polarons and bipolarons. Polarons, with spin of $1/2$ and charge of $\pm e$, are stable in low electric fields, while bipolarons, which are spin-less and possess charge of $\pm 2e$, are very stable in strong fields. More specifically, the increase of voltage has a harmful effect on the structure of polarons, but doesn't have too much effect on bipolarons [19].

Band gap, an important parameter for conducting polymers, is defined as the difference between the highest occupied molecular orbital (HOMO) and the lowest unoccupied molecular orbital (LUMO) [20, 21]. The preferable polymers usually have low band gaps, which is beneficial to energy saving, and some strategies has been adopted for the tune of band gap of conductive polymers by adjusting the structures of the polymers according to the requirement, including planarity, substituents, intermolecular interaction etc., [22, 23].

Among the many methods, (Donor) D- (Acceptor) A approach is an important method in tuning the band gap of polymers, and has been widely used in synthesis of conducting monomers. Electron-rich unit can raise the HOMO energy, making oxidization easy to take place, while electron-deficient unit can lower the LUMO energy level, promoting the reduction of polymers [24, 25]. Electron-deficient units consist of quinoxaline [26], benzotriazole(BTz) [27], benzothiadiazole (BTd) [28, 29], isoindigo [20], diketopyrrolopyrrole [30], benzoselenadiazole (BSe). On the other hand, thiophene and its derivatives is the most common used electron donor unit, such as thiophene (Th), 3,4-ethylenedioxythiophene (EDOT), thieno[3,2-b]thiophene, propylenedioxythiophene (ProDOT) [29].

Youjun He and his co-workers synthesized a poly (thienylene-benzothiadiazole-thienylene-vinylene) with a donor-acceptor configuration, and it has a narrow band gap of 1.50 eV [31]. As an integrated unit, thienylene-benzothiazole-thienylene could be used as an electron-withdrawing substituent for the construction of D-A conjugated polymers. The benzotriazole (BTz) bearing polymers were also designed and synthesized for electrochromic applications. Poly (thiophene-BTz-thiophene) was a simple D-A type polymer, and could switch between all RGB colors, be soluble, p and n-dopable. The copolymerization between BTz and other electron-rich units including benzene, carbazole, fluorene, aryleneethynylene led to the formation of diverse soluble conjugated polymers with variable band gaps and color changes [32]. Very interestingly, the copolymerization between two monomers ProDOT-BTz-ProDOT and ProDOT-BSe-ProDOT gave a valuable polymer with the color switch from neutral black to transmissive (oxidation state), and highlighted the feasibility and great potentials for the application of dual electron deficient units within one polymer backbone for the fine

tune of molecular structure and color changes [33]. As another component of D-A polymers, the electron rich donors also affects the performance of the as prepared polymers in many ways according to their properties, such as electron-donating ability, substituent effect, coplanarity, and among which the high coplanarity is beneficial to increase conjugation degree and high hole mobilities[c,d]. Benzodithiophene and indacenodithiophene are two electron donors with high coplanar structure. Compared with their applications in polymer photovoltaic solar cells, their applications in electrochromic field reserved to be strengthened [34, 35].

In the present study, thienylene-benzothiadiazole-thienylene and thienylene-benzotriazole-thienylene were both taken as the electron acceptor unit, and benzodithiophene or indacenodithiophene was used as the donor unit, and two copolymers were fabricated by the Stille coupling reaction between the above units [36]. Characterization including electrochemistry, spectroelectrochemistry, colorimetry, thermal gravimetric analysis, and kinetic experiments, demonstrated that both copolymers can be good candidates for the potential application in electrochromic fields.

2. EXPERIMENTAL

2.1. Materials

Potassium tert-butoxide (98 %), 1-bromododecane (98 %), hydrobromic acid (48 %), methanol (AR), bis-(triphenylphosphine)palladium (II) chloride ($\text{Pd}(\text{PPh}_3)_2\text{Cl}_2$, 99%), bromine (AR), benzotriazole (AR), N-bromosuccinimide (NBS, 99.0 %), acetonitrile (AR), tetra-n-butylammoniumhexafluorophosphate (TBAPF_6 , 98 %), thiophene, n-butyllithium, tributyltin chloride, tetrahydrofuran, were all purchased from Aladdin Industrial Corporation and used as received. Na_2SO_3 (AR) and MgSO_4 (AR), dichloromethane (DCM, AR), glacial acetic acid (AR), acetone (AR), toluene (AR), ethanol (AR) and chloroform (AR) were bought from Tianjin Chemreagent Co., Ltd.. 1,1'-[4,8-Bis[(2-ethylhexyl)oxy]benzo[1,2-b:4,5-b']dithiophene-2,6-diyl]bis[1,1,1-trimethylstannane](98%) (M1), 1,1'-[4,9,9-tetrakis(4-hexylphenyl)-4,9-dihydro-s-indaceno[1,2-b:5,6-b']dithiophene-2,7-diyl]bis(trimethylstannane) (M2) (99%) were purchased from Derthon Optoelectronic Materials Science Technology Co., Ltd. (Shenzhen, China). 4,7-bis(5-bromo-4-hexylthiophen-2-yl)benzo[c][1,2,5]thiadiazole (M3) and 4,7-bis(5-bromothiophen-2-yl)-2-dodecyl-2H-benzo[d][1,2,3]triazole (M4) were prepared according to our previous reports [37,38].

Indium-tin-oxide (ITO) coated glass (sheet resistance: $< 10 \Omega \cdot \square^{-1}$, Shenzhen CSG Display Technologies, China) was washed with ethanol before use. The electrolyte in our experiments is 0.1 M $\text{TBAPF}_6/\text{ACN}$.

2.2 Instrumentation

^1H NMR and ^{13}C NMR spectra of the products were recorded with a Varian AMX 400 spectrometer in CDCl_3 and tetramethylsilane was internal standard. The electrochemical characteristics were monitored by cyclic voltammetry (CV) using CHI 760 C Electrochemical Analyzer, employing

ITO conducting glass as working electrode, a platinum wire as counter electrode, and an Ag wire as pseudo reference electrode. Spectroelectrochemistry and colorimetry experiments were carried out with a Varian Cary 5000 spectrophotometer and CHI 600 Electrochemical Analyzer. Digital images of the copolymer films were taken with a Canon Power Shot A3000 IS digital camera. Airbrush was used to pattern the copolymer films.

2.3 Synthesis of the monomers

2.3.1. Synthesis of M4

M4 was synthesized according to the previous literature and the synthesis process was showed in Scheme 1 [f]. 2.0 g of 2-dodecyl-4,7-di(thiophen-2-yl)-2H-benzo[d][1,2,3]triazole and 1.89 g of NBS(2.4 equiv) in a mixture of 150 mL of CH₂Cl₂/acetic acid (1:1, v/v) were placed in a flask. The reaction lasted 24 hours under the condition of stir in the darkness. When the reaction was finished, the mixture was poured into 200 mL of deionized water. The organic phase was separated and poured into 100 mL of saturated Na₂SO₃. The extraction was repeated for 4 times, and then distilled the solvent, and column chromatograph was carried out, finally, got the yellow crystallized solid product. ¹H NMR(400 MHz, CDCl₃, δ, ppm) 7.78(d, 2H), 7.48(s, 2H), 7.12(d, 2H), 4.78(t, 2H), 2.17(m, 2H), 1.48-1.15(m, 18H), 0.88(t, 3H)(see Supporting Information Fig. S1a); ¹³C NMR (101 MHz, CDCl₃, δ ppm) 141.62, 141.15, 130.81, 126.88, 122.89, 122.11, 113.10, 56.87, 31.87, 29.99, 29.58, 29.51, 29.40, 29.30, 28.96, 26.52, 22.65, 14.10 (Fig. S1b).

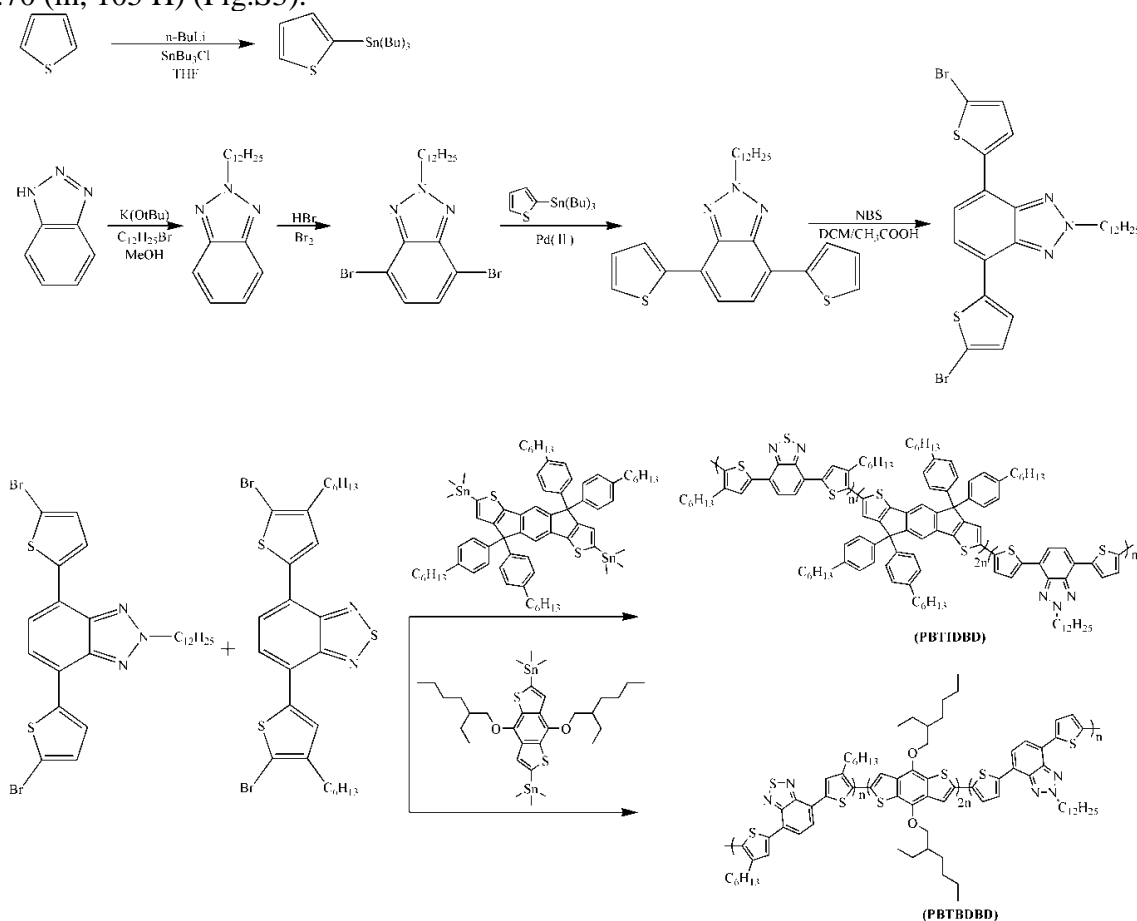
2.3.2. Synthesis of poly(benzotriazole-indacenodithiophene-benzothiadiazole) (PBTIDBD)

The synthetic procedure for PBTIDBD was shown in Scheme 1. 0.7398 g of M2 (1 equiv), 0.1828 g of M4 (0.5 equiv), 0.1880 g of M2 (0.5 equiv), 0.01683 g of Pd(PPh₃)₂Cl₂ and 100 mL of toluene were added to a flask (250 mL) and refluxed for 48 hours under argon atmosphere. After the reaction, it was extracted with methanol and acetone successively for 24 hours, respectively till the solvent in the Soxhlet extractor was transparent. ¹H NMR (400 MHz, CDCl₃) δ 8.08-7.30 (m, 15H), 7.26-7.00 (m, 39H), 3.58 (m, 2H), 2.59 (m, 18H), 1.82-1.40 (m, 22H), 1.40-1.11 (m, 78H), 0.90 (m, 33H) (Fig. S2).

2.3.3. Synthesis of poly(benzotriazole-benzodithiophene-benzothiadiazole) (PBTBDBD)

To a flask, 0.7723 g of M1 (1 equiv), 0.3047 g of M4 (0.5 equiv), 0.3133g of M3 (0.5 equiv), 0.02804 g of Pd (PPh₃)₂Cl₂ and 100mL of toluene were added. The chemical reaction was carried out in argon atmosphere and lasted for 48 hours. When the reaction was finished, the solvent was distilled off under reduced pressure. The crude product was extracted with methanol and acetone successively for 24 hours, respectively, under reflux state in a Soxhlet extractor. When the solution in the Soxhlet extractor was transparent, oligomers and residual catalysts have been removed and the polymer was

purified. $^1\text{H NMR}$ (400 MHz, CDCl_3), δ 8.40-6.50 (m, 14 H), 4.99-3.36 (m, 10 H), 3.00-2.50 (m, 4 H), 2.17-0.70 (m, 105 H) (Fig.S3).



Scheme 1. Synthetic routes of monomers and copolymers of PBTIDBD and PBTBDBD.

3. RESULTS AND DISCUSSION

3.1 Electrochemistry

The copolymer solution was spray casted onto ITO conducting glasses, then be placed in the air until the solvent was evaporated. Electrochemistry experiments were carried out by cyclic voltammetry (CV) using CHI 760 C Electrochemical Analyzer. The voltage was swept from -1.9 V to 1.9 V for PBTIDBD, and -2.0 V to 2.3 V for PBTBDBD. The CV graphs were showed in Fig. 1.

When the voltage sweep to the positive direction, there is a couple of peaks located at 1.75 V and 0.52 V for PBTIDBD, which can be ascribed to p-doping/p-dedoping, while the corresponding peaks for PBTBDBD are at 1.65 V and 0.85 V, lower than PBTIDBD, indicating that PBTBDBD is easier to be oxidized. They have the same electron acceptor units, benzotriazole unit and benzothiadiazole unit, but the electron donor units are different, s-indacenodithiophene for PBTIDBD and benzodithiophene for PBTBDBD. Since benzodithiophene has a more obvious planar structure than indacenodithiophene, leading a better conjugated structure, which is beneficial to the electron delocalization.

As the voltage is negative, there are another couple of peaks at -1.71 V/-1.54 V for PBTIDBD, which was an indication of the n-doping and n-dedoping process. The n-doping/n-dedoping peaks for

PBTBDBD are at -1.71 V/-1.38 V. Electron donor unit can enhance the HOMO energy, promoting oxidation, while electron acceptor unit can lower LUMO energy, making reduction easy. The n-doping potentials are nearly the same, just because they have the same acceptor units [39].

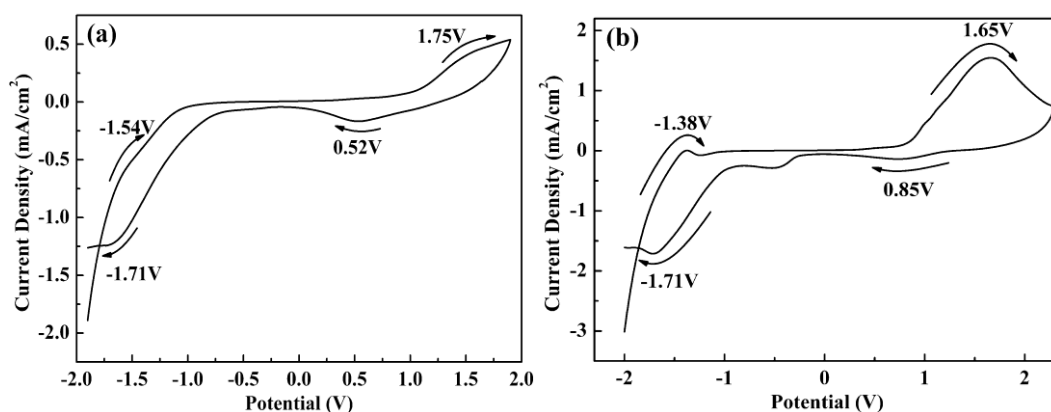


Figure 1. CV of spray coated PBTIDBD film (a) from -1.9 V (Vs., Ag wire) to 1.9 V and PBTBDBD film (b) from -2.0 V to 2.3 V.

3.2. Optical absorption of solution and film

The absorption spectra of two copolymers at the form of solution and solid film were monitored with Varian Cary 5000 spectrophotometer in the visible region. As shown in Fig. 2, the color of the PBTIDBD solution and film are light red and rosybrown, while the color of PBTBDBD solution and film are brownish red and rosybrown. The absorption peak of PBTBDBD is wider than PBTIDBD no matter in solution or in the film form, and PBTBDBD has a more sufficient absorption of short wavelength than PBTIDBD. As seen from Fig. 2(b), the absorption peak of PBTBDBD film nearly covers the whole visible region.

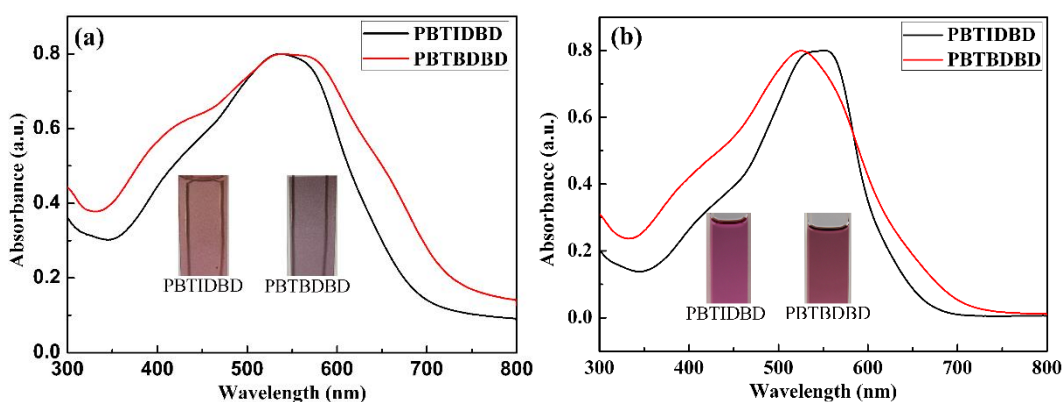


Figure 2. UV-Vis absorption spectra of PBTIDBD and PBTBDBD dissolved in CHCl_3 (a) and those of their films in $\text{TBAPF}_6/\text{CAN}$ (b) in neutral state.

The absorption peaks of PBTBDBD are located at 526 nm for the solution form and 545 nm for the film form. There exists a bathochromic shift, because the π - π stacking in the film is more compact

and can enhance the interchain interaction, extending the conjugation length and lowering the absorption energy finally [40].

The absorption peaks of PBTIDBD are located at 551nm for the solution form and 534nm for the film form. There isn't a red shift, which is contrary to PBTBDBD. Since the coplanar structure of thiophene-phenylene-thiophene could enhance the rigidity, which is beneficial to π - π stacking, so the reason may be ascribed to the tetrahexylaryl groups positioned as peripheral substituents of the backbone. The alkyl side chain is harmful to the intermolecular interaction. Besides, the carbon connecting three phenylenes and one thiophene is sp^3 hybridization, and the four bulk substituents reduce the extent of effective conjugation and co-planarity due to twisting and constrained rotational freedom of the polymer main chains. So the copolymer structure destroys planarity, stretching the distance between adjacent backbones and hindering the π - π stacking.

3.3 Spectroelectrochemistry

Spectroelectrochemistry is an important method for characterizing the resulting copolymers. Fig.3 shows the spectroelectrochemistry of PBTIDBD and PBTBDBD. For PBTIDBD, when the potential is increased from 0 V to 1.2 V, the color of the film turns from rosybrown to light brown, and finally to transparent lightgrey. In neutral state, there is only one absorption peak located at 518 nm, which is a result of π - π^* transition. With the voltage increasing, the initial peak strength decreases, while another two peaks located at 860 nm and 1300 nm appear because of the formation of polarons and bipolarons [41]. Since polaron is unstable under the high potential voltage, which is confirmed by the experiment. When the voltage is up to 1.07 V, the absorption peak of polarons begins to decline. As for bipolarons, the absorption strength increases with the increase of voltage, confirming that bipolarons are relatively stable compared with polarons under high potential voltage.

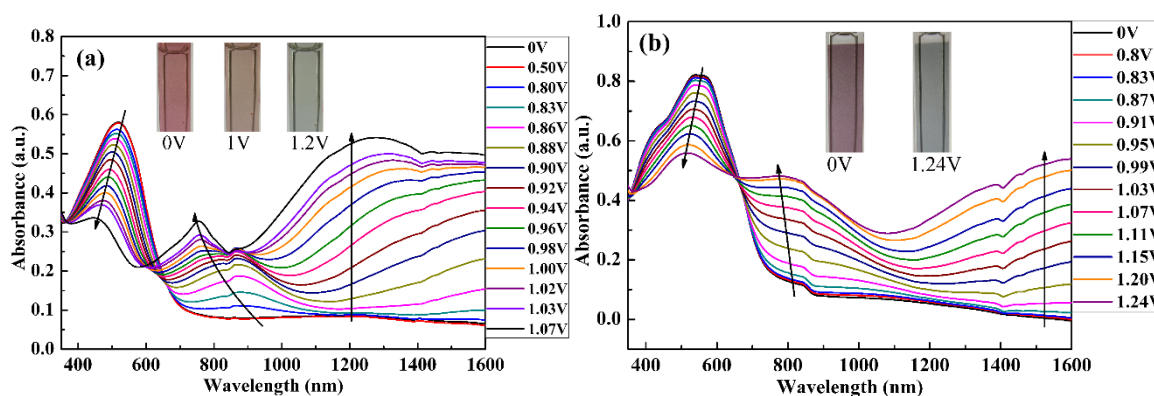


Figure 3. Spectroelectrochemistry of PBTIDBD (a) and PBTBDBD (b) as well as their photos in neutral states and oxidized states. The potential differences were imposed by a potentiostat, and the adsorptions of the films are recorded by spectrometer.

Similar with PBTIDBD, PBTBDBD shows the same trend. When the copolymer is at 0 V, there is only an absorption peak at 540 nm. As the voltage increases, the primitive absorption peak turns down, and two new peaks at 780 nm and 1400 nm appear corresponding to the polarons and

bipolarons. There is one isosbestic point at 667 nm as shown in Fig. 3(B), for PBTBDBD. The color turns from rosybrown to transparent grey from neutral state to oxidized state.

According to the cyclic voltammetry experiments, and spectroelectrochemistry experiments, we can calculate some parameters, as summarized in Table 1, including onset oxidation potential (E_{onset}), onset of the optical absorption spectra in neutral states (λ_{onset}), maximum absorption wavelength in solution (λ_{max} , solution) and film (λ_{max} , film) morphology, optical band gap (E_g) and HOMO/LUMO energy levels. The E_g , E_{HOMO} and E_{LUMO} are calculated as the formula $E_g = 1241/\lambda_{\text{onset}}$, $E_{\text{HOMO}} = -e(E_{\text{onset}} + 4.4)$ and $E_{\text{LUMO}} = E_{\text{HOMO}} + E_g$, respectively [41].

Table 1. The parameters including E_{onset} , λ_{onset} (film), λ_{max} (solution), λ_{max} (film), E_g and HOMO/LUMO energy levels of PBTIDBD and PBTBDBD.

copolymers	E_{onset} V	λ_{onset} (film) nm	λ_{max} (solution) nm	λ_{max} (film) nm	E_g eV	HOMO eV	LUMO eV
PBTIDBD	1.06	668	551	534	1.86	-5.46	-3.60
PBTBDBD	0.81	738	526	545	1.68	-5.21	-3.53

The band gap, related to energy difference between the lowest level of the conduction band and the highest level of valence band, is a very important parameter for conducting polymers. The band gap of PBTIDBD is 1.86 eV, while the band gap of PBTBDBD is 1.68 eV. Both band gaps are relatively low, the reason is that they were copolymerized with three monomers, especially two electron deficient units, which is beneficial to reducing band gap. The reason why the band gap of PBTBDBD is smaller than PBTIDBD is that the coplanarity of benzodithiophene is higher than that of the indacenodithiophene, which is beneficial to π - π^* transition, reducing the energy transition.

Moreover, as noticed that, the LUMO values of both polymers are -3.60 eV and -3.53 eV, and the difference is negligible. While the HOMO values of both copolymers are -5.46 eV and -5.21 eV, the difference is as high as 0.25 eV. Since benzodithiophene and s-indacenodithiophene are taken as donor units and donor units make a contribution to enhancing the HOMO energy, so we get the conclusion that benzodithiophene is more effective than s-indacenodithiophene in reducing the band gap as the donor unit.

3.4 Electrochromic switching of both copolymers

For electrochromic polymers, the high optical contrasts (OC) are indispensable for energy-saving smart window. The OC value ($\Delta T\%$) is defined as the transmittance difference between neutral state and oxidized state determined at the maximum absorption peak. The electrochromic switching of both copolymers at different wavelengths are shown in Fig. 4.

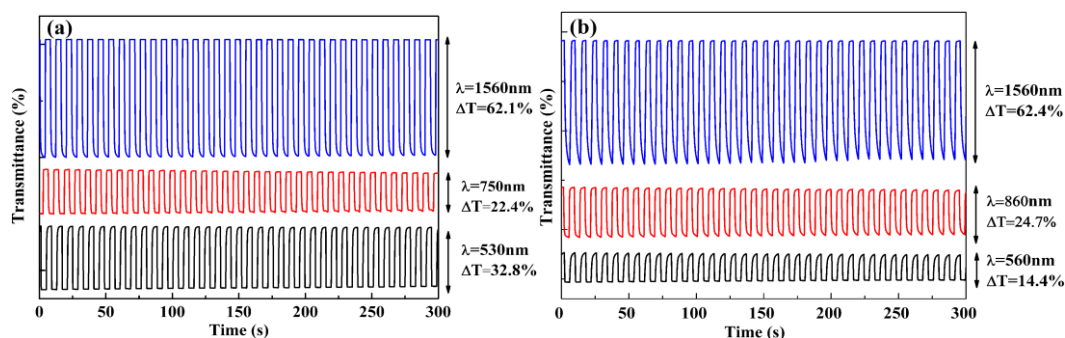


Figure 4. Electrochromic switching of PBTIDBD(a) between 0 V to 1.40 V and PBTBDBD (b) between 0 V and 1.40 V. The potential differences were imposed by a potentiostat, and the transmittance changes of the films are recorded by spectrometer.

For PBTIDBD, when the voltage is inter-switched between 0 V and 1.40 V, the optical contrasts are 32.8% at 530 nm, 22.4% at 750 nm, and 62.1% at 1560 nm. While for PBTBDBD, the optical contrasts are 14.4 % at 560 nm, 24.7% at 860 nm and 62.4% at 1560 nm when the voltage is interchanged between 0 V and 1.40 V. Both copolymers exhibit high optical contrast, so they can show significant color change.

Besides, we can also calculate the response time (RT) ($t_{95\%}$) according to Fig. 4. RT value is defined as the 95% of the full switch time from neutral state to oxidized state for the human eyes, which are not so sensitive to color change [42]. The RT of PBTIDBD are 0.95 s at 530 nm, 0.84 s at 750 nm, 1.04 s at 1560 nm, while the RT of PBTBDBD are 2.40 s at 560 nm, 1.54 s at 860 nm, and 2.68 s at 1560 nm. No matter in visible region, or in near infrared region, the RT of PBTIDBD are much shorter than of PBTBDBD. Because the tetrahexylaryl groups positioned as peripheral substituents of the s-indacenodithiophene unit in PBTIDBD are very large and when they twist, it's unbeneficial to π - π stacking, resulting less compact film. The less compact film could facilitate ion-solvent ingress and egress, so the time is short.

The coloration efficiency (CE) (η) is used to appraise the amount of energy to affect color change and is defined as the ratio of the change in optical density to the charge density, and the equations are showed as follows [43].

$$\eta = \Delta OD / \Delta Q$$

$$\Delta OD = \lg(T_b / T_c)$$

$$\Delta Q = Q / A$$

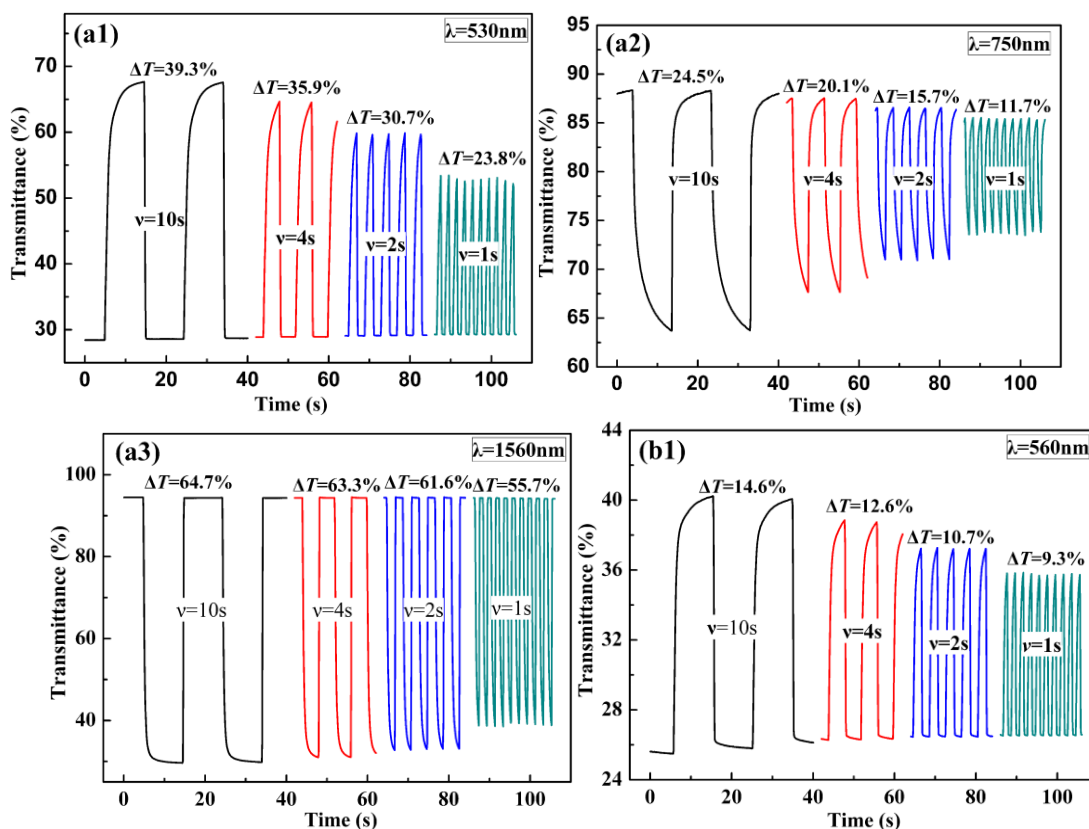
Where the unit of coloration efficiency is $\text{cm}^2 \cdot \text{C}^{-1}$, T_b , T_c are transmittances in neutral states and oxidized states, respectively. Q is integrated from the multi-potential steps diagram, where current varies with time. A donates the area of the film.

The coloration efficiencies of PBTIDBD are $186.58 \text{ cm}^2 \cdot \text{C}^{-1}$ at 530 nm, $64.18 \text{ cm}^2 \cdot \text{C}^{-1}$ at 750nm, $276.29 \text{ cm}^2 \cdot \text{C}^{-1}$ at 1560 nm, while the coloration efficiencies of PBTBDBD are $86.34 \text{ cm}^2 \cdot \text{C}^{-1}$ at 560 nm, $91.84 \text{ cm}^2 \cdot \text{C}^{-1}$ at 860 nm, $193.31 \text{ cm}^2 \cdot \text{C}^{-1}$ at 1560 nm. There is larger coloration efficiency in near infrared region than in the visible region for both of the polymers. The coloration efficiency of PBTIDBD is higher than that of PBTBDBD. Table 2 summarizes the electrochromic switching parameters of PBTIDBD and PBTBDBD including OC, RT and CE.

Table 2. The electrochromic switching of PBTIDBD and PBTBDBD.

copolymers	λ	$\Delta T\%$	RT ($t_{95\%}$)	CE (η)
	nm	%	s	$\text{cm}^2 \cdot \text{C}^{-1}$
PBTIDBD	530	32.8	0.95	186.58
	750	22.4	0.84	64.18
	1560	62.1	1.04	276.29
PBTBDBD	560	14.4	2.40	86.34
	860	24.7	1.54	91.84
	1560	62.4	2.68	193.31

We also measured the optical contrasts at different intervals, including 10 s, 4 s, 2 s and 1 s. For PBTIDBD, when the interval is changed from 10 s to 1 s, copolymers maintain 23.8% OC value at 530 nm with a 39.44% decrease (Fig. 5a1), an 11.7% OC value at 750 nm at 1 s with a 52.3% drop (Fig. 5a2), and 55.7% OC value at 1560 nm with a 13.91% decrease (Fig.5a3). While for PBTBDBD, when the interval is changed from 10 s to 1 s, copolymers maintained a 9.3% OC value at 560 nm with a 36.3% decrease (Fig.5b1), a 16.1% OC value at 860 nm with 33.74% drop (Fig.5b2), and 47.1% OC value at 1560 nm with a 21.63.0% decrease (Fig.5b3). Both copolymers exhibit significant decline, so if we want to acquire a high optical contrast, the interval should not be too small.



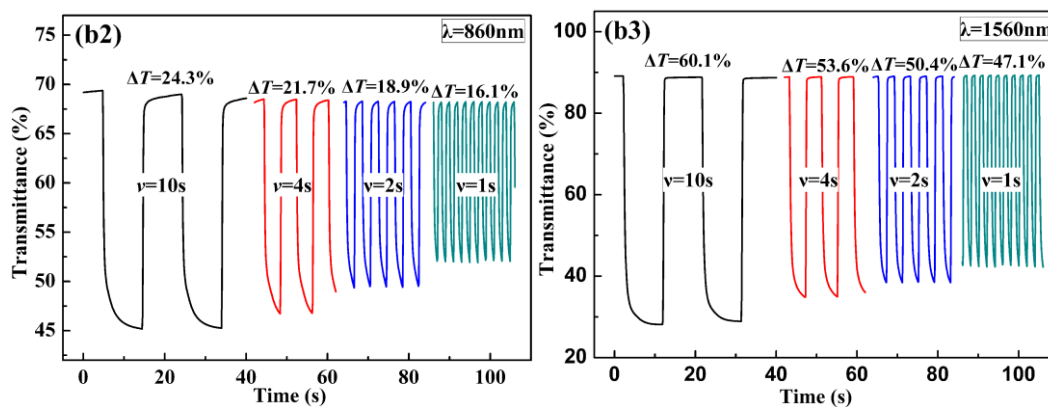


Figure 5. Electrochromic switching of PBTIDBD (a₁, a₂, a₃) and PBTBDBD (b₁, b₂, b₃) with an interval of residence time s of 10 s, 4 s, 2 s and 1 s in the multi-step potential measurement, and the transmittance changes are recorded by the spectrometer.

3.5 Colorimetry

Colorimetry is an effective method to evaluate the color of copolymers at different potentials and in our experiment, the CIE 1976 $L^*a^*b^*$ color space was adopted to assess the color of copolymers at different voltages. L^* signifies the lightness from 0 to 100, a^* represents the ratio red versus green, and b^* means how much yellow versus blue [42,43].

For PBTIDBD, as shown in Fig. 6a1, when the voltage increases, the lightness keeps stable until 1.0 V, then a dramatic increase appears, finally there is another platform. When the copolymers turn from neutral state to oxidized state, the lightness turns brighter, in other words, the copolymer film changes transparent and light. As for a^* and b^* (Fig. 6a2), the copolymers turn from red to green, and from blue to yellow. As a result, the copolymers turn from rosybrown in neutral state to transparent lightgrey in oxidized state.

Similar with PBTIDBD, as shown in Fig.6b1, when the potential increases, the lightness of PBTBDBD firstly keeps steady, and then when the voltage is up to 0.8 V, it begins to climb to a higher value. When it changes from neutral state to oxidized state, a^* changes from red to green, and b^* changes from blue to yellow (Fig.6b2). In consideration with three factors, the color of copolymers changes from rosybrown in neutral state to transparent grey in oxidized state.

In addition, the film thickness also plays an important role in tuning the color of the film. With the film thinner, the lightness turns higher, so we can tune the thickness to realize the color change. As the film thickness of PBTBDBD was changed from 0.19 a.u. to 0.41 a.u. and finally to 0.70 a.u. (measured at 560 nm), the lightness changes from 97.9 to 92.6 and to 77.3 in neutral state (Fig.6b1). The enhancement is significant, so it's also a valid method to tune the lightness of film.

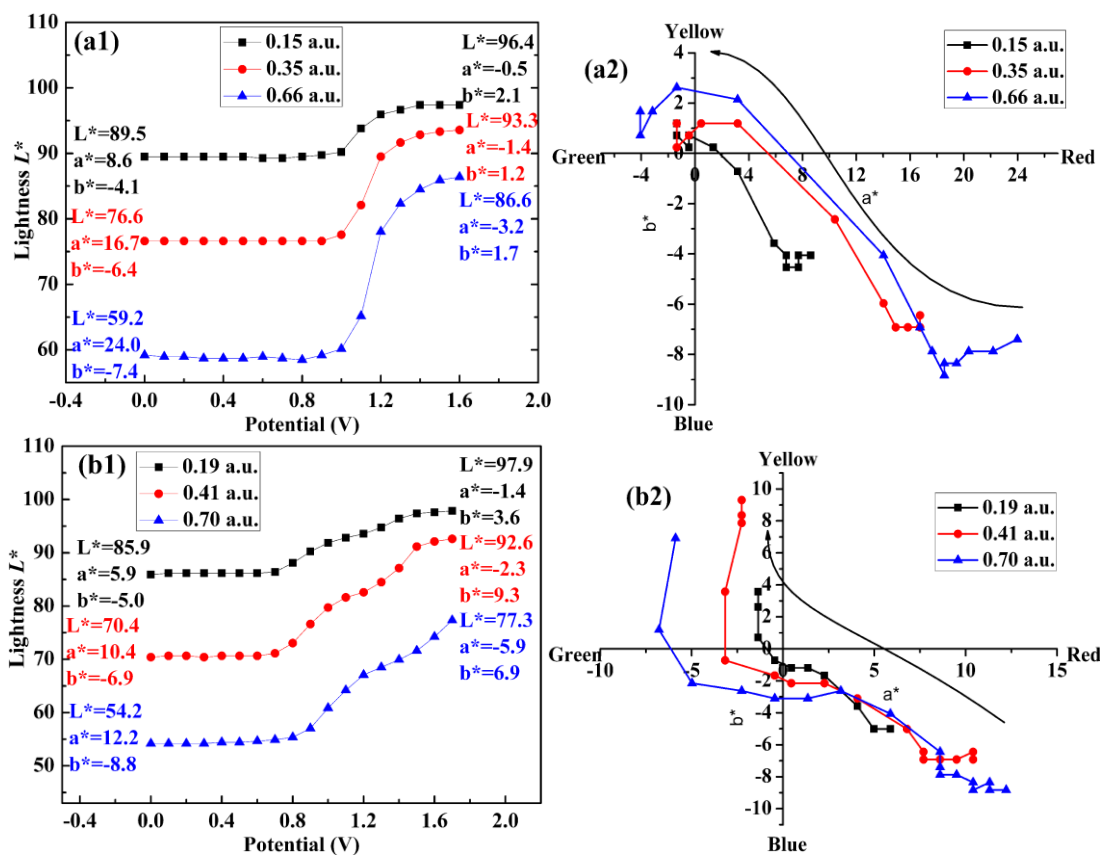


Figure 6. Colorimetry of PBTIDBD (a₁, a₂) and PBTBDBD (b₁, b₂). The potential differences were imposed by a potentiostat and the colorimetry changes are recorded by the spectrometer.

3.6. Thermal gravimetric analysis

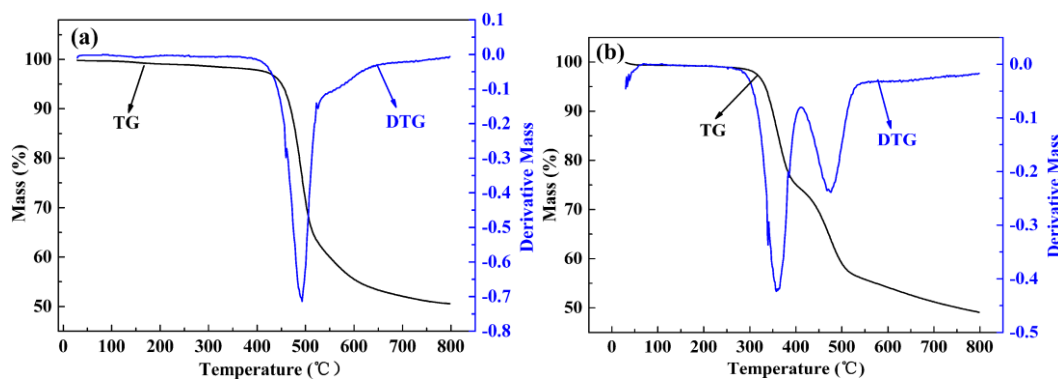


Figure 7. Thermal gravimetric analysis of PBTIDBD (a) and PBTBDBD (b). TG refers to the loss in mass percentage as the function of temperature, and the DTG curve was the first differential curve of TG to temperature.

Thermal stability is also necessary if the copolymers are applied to the reality. We hope the copolymers could keep stable even at a high temperature. Thermal gravimetric analysis is used to measure the mass loss varied with temperature. As shown in Fig. 7, PBTIDBD begins to decompose at 463 °C, and PBTBDBD begins to decompose when the temperature is 326 °C. Both copolymers are

stable at a high temperature. Especially for PBTIDBD, the decomposition temperature is much higher than PBTBDBD. This may be because of that the repeating unit of PBTIDBD contains more phenyleneblocking unit than PBTBDBD repeating unit and the condensed aromatics degree is much higher. The higher aromatic structure and the longer side chain may explain the phenomenon well [43].

4. CONCLUSION

Two copolymers were copolymerized and characterized through electrochemistry, spectroelectrochemistry, kinetic experiments and thermal gravimetric analysis. They both have relatively low band gap, 1.86 eV for PBTIDBD, and 1.68eV for PBTBDBD. The benzodithiophene has a better coplanarity than s-indacenodithiophene. The OC of both copolymers in near infrared region are 62.1% and 62.4 %, respectively, demonstrating good potential in near infrared application. The RT of both polymers are 1.04 s and 2.68 s at long wavelength, and the CE of both copolymers are $276.29 \text{ cm}^2 \cdot \text{C}^{-1}$ and $193.91 \text{ cm}^2 \cdot \text{C}^{-1}$ at long wavelength. The problem we met in the experiments is the poor solubility, so copolymers with high solubility have enormous potential for the future application. Both copolymers can be good candidates in electrochromic polymers application.

ACKNOWLEDGEMENTS

This work was financially supported by the National Natural Science Foundation of China (51473074 and 21601079), and Natural Foundation of Shandong Province (ZR2016EMQ06).

SUPPORTING INFORMATION

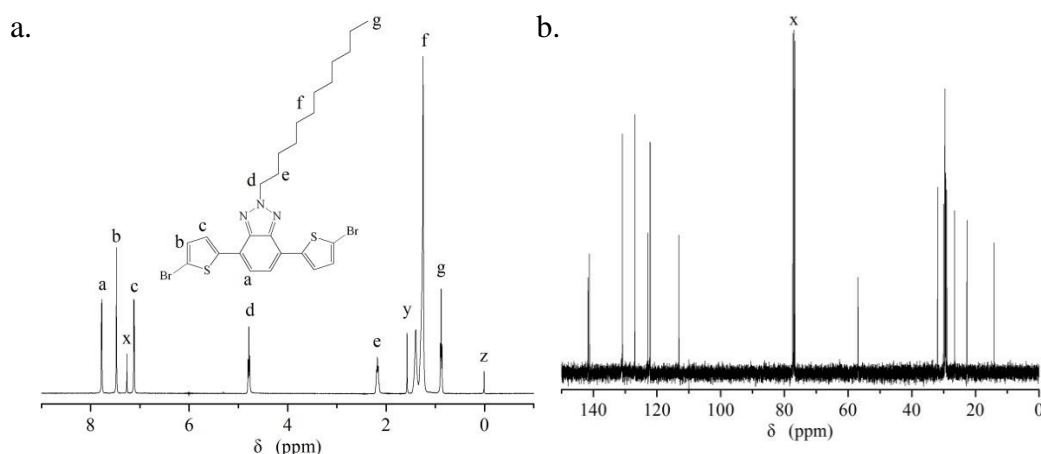


Fig. S1. (a) ^1H NMR spectrum and (b) ^{13}C NMR spectrum of 4,7-bis(5-bromothiophen-2-yl)-2-dodecyl-2H-benzo[d][1,2,3]triazole in CDCl_3 , x, y, z denote the peaks of chloroform, water and tetramethylsilane.

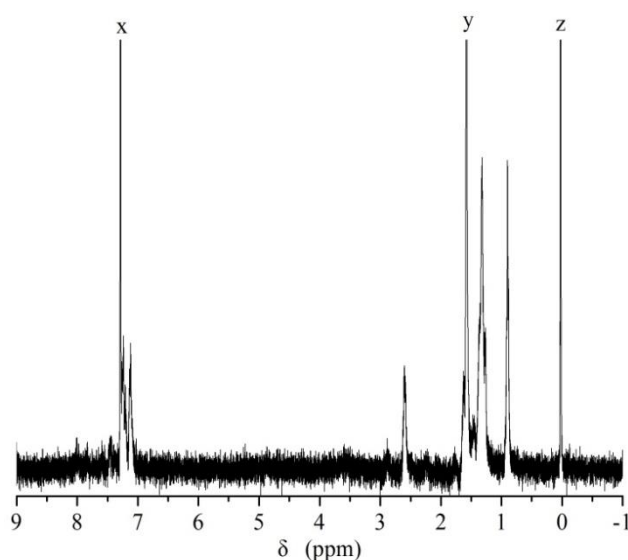


Fig. S2. ^1H NMR spectrum of **PBTIDBD** in CDCl_3 , x, y, z donate the peaks of chloroform, water and tetramethylsilane.

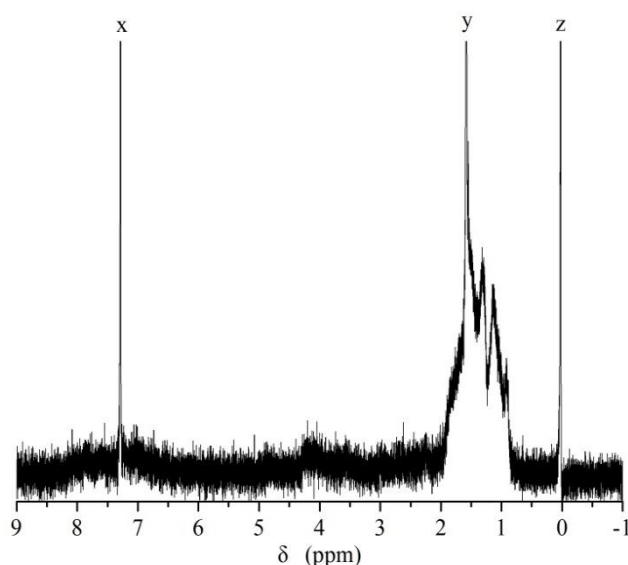


Fig. S3. ^1H NMR spectrum of **PBTBDBD** in CDCl_3 , x, y, z donate the peaks of chloroform, water and tetramethylsilane.

References

1. D.T. Christiansen, D. L. Wheeler, A. L. Tomlinson, J. R. Reynolds, *Polym. Chem.*, 9 (2018) 3055.
2. M. Herrera, A.M. Mohammad, M. A. Mahmoud, *ACS. Appl. Nano. Mater.*, 2 (2018) 577.
3. C.L. Chochos, R. Singh, V.G. Gregoriou, M. Kim, A. Katsouras, E. Serpetzoglou, I. Konidakis, E. Stratakis, K. Cho, A. Avgeropoulos, *ACS. Appl. Mater. Inter.*, 10 (2018) 10236.
4. J.Tagare, S.Vaidyanathan, *J. Mater. Chem. C*, 6 (2018) 10138.
5. Y. L. Ma, Z. J. Kang, Q. D. Zheng, *J.Mater. Chem. A.*, 5 (2017) 1860.
6. B. H. Chen, S.Y. Kao, C.W. Hu, M. Higuchi, K.C. Ho, Y.C. Liao, *ACS. Appl. Mater. Inter.*, 7 (2015) 25069.
7. W. H. Nguyen, C.J. Barile, M.D. McGehee, *J. Phys. Chem. C.*, 120 (2016) 26336.
8. R.H. Bulloch, J.A. Kerszulis, A.L. Dyer, J.R. Reynolds, *ACS. Appl. Mater. Inter.*, 6 (2014) 6623.
9. R.J. Mortimer, K.R. Graham, C.R.G. Grenier, J.R. Reynolds, *ACS Appl. Mater. Inter.*, 1 (2009) 2269.

10. P. J. Shi, C.M. Amb, A.L. Dyer, J.R. Reynolds, *ACS Appl. Mater. Inter.*, 4 (2012) 6512.
11. J. Lee, A.J. Kalin, C.X. Wang, J. T. Early, A.H. Mohammed, L. Fang, *Poly. Chem.*, 9 (2018) 1603.
12. C.M. Amb, A.L. Dyer, J.R. Reynolds, *Chem. Mater.*, 23 (2011) 397.
13. J. Li, J. P. He, *ACS Macro Lett.*, 4 (2015) 372.
14. C. D. Grande, M.C. Tria, G.Q. Jiang, R. Ponnappati, R. Advincula, *Macromolecules.*, 44 (2011) 966.
15. W. Z. Monika, J. Goclon, A. Basa, K. Winkler, *J. Phys. Chem. C.*, 122 (2018) 25539.
16. C. S. Juna, S. H. Kwona, H. J. Choia, Y. Seo, *ACS Appl. Mater. Inter.*, 9 (2017) 44811.
17. Y. Chen, S. Zeng, J.F. Qian, Y.D. Wang, Y. L. Cao, H. X. Yang, X. P. Ai, *ACS Appl. Mater. Inter.*, 6 (2014) 3508.
18. N.S. Sariciftci, L. Smilowitz, C. Zhang, V.I. Srdanov, A.J. Heeger, F. Wudl, *Appl. Phys. Lett.*, 62 (1993) 585.
19. G.M.E. Silva, P.H. Acioli, *J. Mol. Struct.*, 539 (2001)45.
20. H. H. Xie, M. Wang, L.Q. Kong, Y. Zhang, X. P. Ju, J.S. Zhao, *RSC Adv.*, 7 (2017) 11840.
21. W.L. Zhuang, A. Lundin, M.R. Andersson, *J. Mater. Chem A*, 2 (2014), 2202.
22. X. F. Cheng, X. P. Ju, H. M. Du, Y. Zhang, J.S. Zhao, Y. Xie, *RSC Adv.*, 8 (2018) 23119.
23. Y. Zhang, L.Q Kong, X.P Ju, H.M. Du, J.S Zhao, Y. Xie , *RSC Adv.*, 8 (2018) 21252.
24. Z. Xu, M. Wang, J.S. Zhao, C.C. Cui, W.Y. Fan, J. F. Liu, *Electrochim. Acta.*, 125 (2014) 241.
25. D. Zhang, M. Wang, X.L. Liu, J.S. Zhao, *RSC Adv.*, 6 (2016) 94014.
26. H. Zhao, Y.Y. Wei, J.S. Zhao, M. Wang, *Electrochim. Acta.*, 146 (2014) 231.
27. C.L. Wang, M. Wang, Y. Zhang, J.S. Zhao, C.G Fu, *RSC Adv.*, 6 (2016) 80002.
28. W.S. Li, Y.T Guo, J. J. Shi, H.T. Yu, H. Meng, *Macromolecules.*, 49 (2016) 7211.
29. P. Thongkasee, A. Thangthong, N. Janthasing, T. Sudyoosuk, S. Namuangruk, T. Keawin, S. Jungstittiwong, V. Promarak, *ACS Appl. Mater. Inter.*, 6 (2014) 8212.
30. W.T. Neo, Q. Ye, Z.G. Shi, S.J.Chuaac, J.W. Xu, *Mater. Chem. Front.*, 2 (2018) 331.
31. Y.J. He, G.J. Zhao, J.Min, M.J. Zhang, Y.F. Li, *Polymer.*, 50 (2009) 5055.
32. A. Balan, D. Baran, L. Toppare. *Polym. Chem.*, 2 (2011)1029.
33. M. İçli, M. Pamuk, F. Algi, A.M. Önal, A. Cihaner, *Org. Eletron.*,11(2010) 1255.
34. C. Liang, H.Q. Wang, *Org. Electron.*, 50 (2017) 443.
35. X.L. Liu, L.Q. Kong, H.M. Dou, Y. Zhang, J.S. Zhao, Y. Xie. *Org. Electron.*, 64(2019) 223.
36. C.L. Chochos, S.A. Choulis, *Prog. Polym. Sci.*, 36 (2011), 1326.
37. J.Z. Xu, Q. Ji, L.Q. Kong, H.M. Dou, X. P. Ju, J.S. Zhao, *Polymers.*, 9(2018) 450.
38. G. Hızalan, A. Balan, D. Barana, L. Toppare, *J. Mater. Chem.*, 21(2011) 1804.
39. M.I. Ozkut, M. P. Algi, Z. Öztas, F. Algi, A. M. Önal, A. Cihaner, *Chem. Mater.*, 22 (2010) 4034.
40. W. T. Neo, L.M. Loo, J. Song, X.B. Wang, C.M. Cho, H.S.O. Chan, Y. Zong, J.W. Xu, *Poly. Chem.*, 49 (2013) 2446.
41. X.J. Song, M. Wang, L. Q. Kong, J.S. Zhao, *RSC Adv.*, 7 (2017) 18189.
42. J. Jensen, M. Hösel, I. Kim, J.S. Yu, J. Jo, F.C. Krebs, *Adv. Fun. Mater.*, 24 (2014) 1228.
43. S. Chen, D. Zhang, M. Wang, L.Q Kong, J.S. Zhao, *New J. Chem.*, 40 (2016) 2178.